Experimental Observations of Dynamic Critical Phenomena in a Lipid Membrane

Aurelia R. Honerkamp-Smith, Benjamin B. Machta, and Sarah L. Keller

Phys. Rev. Lett. **108**, 265702 — Published 28 June 2012

DOI: 10.1103/PhysRevLett.108.265702

Experimental observations of dynamic critical phenomena in a lipid membrane

Aurelia R. Honerkamp-Smith,[1] Benjamin B. Machta,[2] and Sarah L. Keller[1,*]

[1]*Department of Chemistry, University of Washington, Seattle WA 98195-1700*
[2]*Department of Physics, Cornell University, Ithaca NY 14850*

Near a critical point, the time scale of thermally-induced fluctuations diverges in a manner determined by the dynamic universality class. Experiments have verified predicted 3D dynamic critical exponents in many systems, but similar experiments in 2D have been lacking for the case of conserved order parameter. Here we analyze time-dependent correlation functions of a quasi-2D lipid bilayer in water to show that its critical dynamics agree with a recently predicted universality class. In particular, the effective dynamic exponent $z_{\rm eff}$ crosses over from ~ 2 to ~ 3 as the correlation length of fluctuations exceeds a hydrodynamic length set by the membrane and bulk viscosities.

PACS numbers: 64.60.Ht, 68.35.Rh, 87.16.D-, 87.16.dt

Lipids self-assemble in water to form sheets that are two molecules thick, within which the lipids are free to diffuse. When composed of several lipid species these two-dimensional (2D) liquid membranes can demix into coexisting liquid phases, termed $L_{\rm o}$ and $L_{\rm d}$, over a range of temperatures and compositions, and can exhibit critical behavior [1–4]. Among 2D critical phenomena, composition fluctuations in membranes are rather unique in that their large sizes and long decay times are accessible to optical microscopy. For example, Fig. 1 and supplementary movies show a vesicle (a spherical membrane shell) in which correlated regions reaching 10 μm persist for seconds [5]. Direct visualization of these equilibrium fluctuations has recently been used to show that *static* critical exponents for lipid membranes are consistent with the 2D Ising universality class [3, 6]. Here we exploit the ability to visualize *dynamics* of these fluctuations to examine for the first time the dynamic critical phenomena in this system. We find that although the statics are 2D phenomena, the critical dynamics are modified by hydrodynamic coupling to the surrounding 3D fluid.

Static critical exponents, which describe how observables such as correlation length vary as the critical point is approached, are identical for all systems in a given universality class, independent of their detailed microscopic physics [7, 8]. For example, although membranes have a conserved order parameter and ferromagnets do not, membranes exhibit static exponents $\nu = 1.2 \pm 0.2$ and $\beta = 0.124 \pm 0.03$, consistent with the expected 2D Ising values of $\nu = 1$ and $\beta = 1/8$ [3]. Results in plasma membrane vesicles are also consistent with 2D Ising exponents $\nu = 1$ and $\gamma = 7/4$ [6]. Systems that are in the same static universality class can fall into different dynamic universality sub-classes determined by conservation laws constraining how fluctuations dissipate [9]. The critical exponent z for each dynamic subclass quantitatively describes the scaling of the dynamics. It relates how the correlation time τ_s diverges as temperature T approaches the critical temperature T_c, such that $\tau_s \propto |(T - T_c)/T_c|^{-\nu z}$ where ν is the static critical exponent. Experiments measure an effective exponent $z_{\rm eff}$ that approaches z as $T \to T_{\rm c}$ and $\xi \to \infty$. Dynamic sub-classes relevant to 2D systems with conserved order parameter are notable equally for their wealth of theoretical predictions [9–11] and for the lack of experiments that systematically test those predictions.

Only a few previous measurements of dynamic critical exponents in 2D systems exist. Most experiments have been conducted on magnetic films. Using ferromagnetic films of $\sim$ two monolayers, Dunlavy and Venus found $\nu z = 2.09 \pm 0.06$, with $\nu = 1$ [12]. Fewer experiments have been conducted on systems with conserved order parameter. Careful attempts to measure z were made in thin films of lutidine and water, but were unable to reach the 2D critical regime [13]. In plasma membrane vesicles from living rat basophil leukemia cells, fluctuation decay times were reported to be consistent with $z \approx 2$ [6].

Here we obtain $z_{\rm eff}$ as T approaches $T_{\rm c}$ in a lipid membrane surrounded by water and compare to theory recently developed for an analogous system: a 2D critical binary fluid embedded in a non-critical bulk fluid [10, 11].

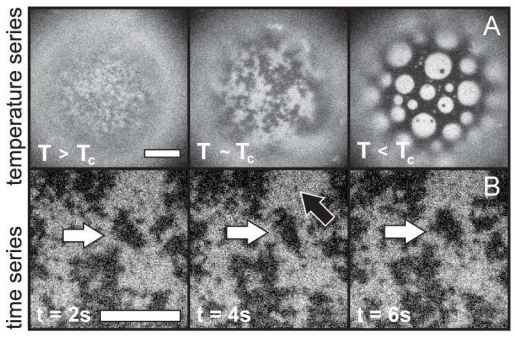

FIG. 1: Fluorescence micrographs of vesicles of diameter 200 μm. (A) As temperature changes from $T > T_{\rm c}$ ($T = 31.25^{\circ}$C, $T_{\rm c} \approx 30.9$) to $T \sim T_c$ ($T = 31.0^{\circ}$C) fluctuations in lipid composition grow. Below T_c, at $T = 28^{\circ}$C, domains appear. Scale bar = 10 μm. (B) A movie of composition fluctuations within a vesicle above $T_{\rm c}$. Large fluctuations persist for seconds (white arrows), whereas small ones disappear by the next frame (black arrow). Scale bar = 20 μm.

This new theory incorporates three essential features of lipid bilayer dynamics: conserved order parameter, collective hydrodynamics, and hydrodynamic coupling between the bilayer and bulk [10, 11]. Inclusion of only the first feature within an Ising model yields Model B, in which composition fluctuations dissipate through diffusion of microscopic constituents [9]. 2D Model B predicts $z = 4 - 2\beta = 3.75$ [9], and numerical schemes give $z = 3.80$ and $z = 3.95$ [14, 15]. Inclusion of the first *two* features, such that collective hydrodynamic motion replaces single particle diffusion as the dominant mechanism of order parameter relaxation, yields Model H. 2D Model H with coupling to only 2D momentum modes predicts $z \approx 2$ [9]. Inclusion of all *three* features yields Model HC, where HC denotes hydrodynamic coupling of the membrane to the bulk. This new version extends Model H to account for modes in both the 2D membrane and the 3D bulk fluid, with the result that $z = 3$ [10, 11].

Intuition for the role of the coupling between the membrane and bulk within Model HC can be gleaned from an approximation for 3D Model H by Kawasaki [16]. Critical fluctuations are treated as spherical inclusions of diameter ξ that diffuse a distance ξ to equilibrate [9, 16–18]. As such, correlation time varies as $\tau \sim \xi^2/D(\xi)$, where $D(\xi)$ is the inclusion's diffusion constant in a non-critical fluid. In 3D, $D(r) \sim 1/r$, where r is the inclusion's radius. Using $\tau \propto |(T - T_c)/T_c|^{-\nu z} \propto \xi^z$ yields $z \approx 3$. A more sophisticated theoretical treatment gives $z = 3.065$ [18]. Applying the same reasoning to 2D Model H, in which diffusion of inclusions has only a logarithmic dependence on r, yields $z \approx 2$. Again, more sophisticated treatments produce similar values; see [5] for more detail. This argument can be extended to predict the value z should take in a 2D critical system embedded in a bulk fluid. Classic work by Saffman and Delbrück examined diffusion of an inclusion in a 2D liquid of viscosity η_{2D} immersed in a bulk fluid of 3D viscosity η_{3D}, where hydrodynamic length $L_h = \eta_{2D}/\eta_{3D}$ is an important parameter [19, 20]. When $r \gg L_h$, dissipation is primarily into the bulk and $D(r) \propto 1/r$ as in 3D Model H. When $r \ll L_h$, dissipation is primarily into 2D hydrodynamic modes and $D(r) \propto \ln(L_h/r)$, similar to 2D Model H. Two groups have independently noted that when L_h is considered, z_{eff} for a 2D critical binary fluid embedded in bulk liquid crosses over from $z_{eff} \approx 2$ when $\xi \ll L_h$ to $z_{eff} \approx 3$ when $\xi \gg L_h$ [10, 11].

The next four paragraphs demonstrate that experimental results here are in excellent agreement with the recent predictions of Model HC, namely that z_{eff} crosses over from ~ 2 to ~ 3 as $T \to T_c$ and $\xi \to \infty$. Further experimental details follow the results.

A time series of the order parameter, $m(r,t)$, was extracted from videos of vesicles collected via fluorescence microscopy. For membranes, $m(\vec{r})$ is the deviation from average composition as reported by an image's pixel grey scales. A time-correlation function $C(r,\tau)$, and its Fourier transform in space, the structure factor $S(k,\tau)$, were calculated for each wavenumber k.

Curves of $S(k,\tau)/S(k,0)$ vs $k^{z_{eff}}\tau$ were plotted for a range of z_{eff} values. Fig. 2B illustrates how the correct z_{eff} was identified: for a single value of z_{eff}, all experimentally-measured curves at different k values (Fig. 2A) collapsed most fully onto a single curve, here at $z_{eff} = 2.8 \pm 0.2$. Fig. 3A shows z_{eff} values extracted in this manner from data over the entire measurable range of correlation lengths. In Fig. 3A, z_{eff} rises from from near 2 to near 3 as $T \to T_c$, in accord with Model HC [10, 11].

Fig. 2C-D validates this method by showing that standard simulations of Model B Kawaski dynamics that are blurred to mimic experimental limitations and then analyzed in the same way as the experimental data give $z = 3.6 \pm 0.2$ in agreement with the expected value of $z = 3.75$ (see [5] for details). Simulations were run on a 400x400 bi-periodic square lattice. Blur was achieved by averaging snapshots over 200 consecutive Monte Carlo sweeps, leaving a break of 800 sweeps without snapshots, and repeating the process, which reproduced the effects of a camera shutter opening for 100 ms of every 500 ms.

Excellent agreement between predicted and measured structure factors provides even stronger evidence that Model HC describes critical dynamics in membranes. Inaura and Fujitani give a prediction for the entire time-

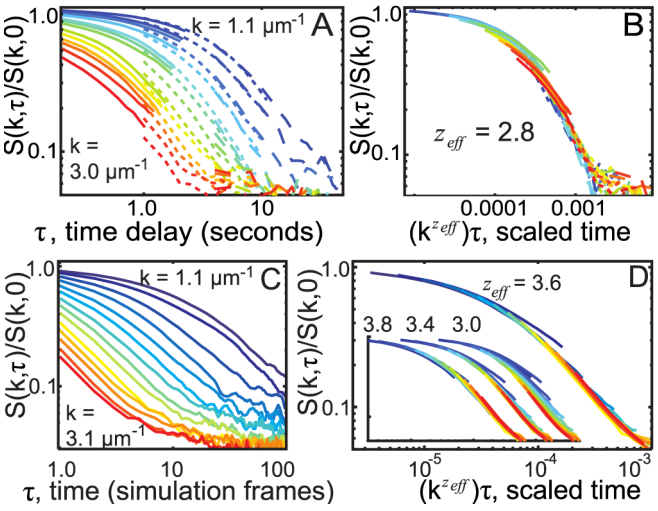

FIG. 2: (color online). (A and B) Rescaling experimental data closest to T_c by $k^z\tau$ collapses all curves to $z_{eff} = 2.8$, consistent with Model HC. Normalized structure factors are shown for $\xi = 13 \pm 2.2$ μm and three video rates: 10 frames per second (fps, solid lines), 2 fps (short dash), and 0.5 fps (long dash). Colors denote wavenumbers $k = 1.1$ μm^{-1} (top curve, blue) to 3.0 μm^{-1} (bottom, red). (C and D) Simulations solely to verify technique. Structure factors of Kawasaki dynamics at $T = T_c$ blurred in time to mimic experimental limitations collapse at $z_{eff} = 3.6 \pm 0.2$, consistent with $z = 3.75$ for 2D Model B. Colors range from $k = 1.1$ μm^{-1} to 3.1 μm^{-1}. Insets show collapses used to determine bounds for z_{eff} and failure of collapse at $z_{eff} = 3$.

dependent structure factor $S(k,\tau)$ for Model HC, taking as input η_{2D}, η_{3D}, and a mean-field approximation for the static structure factor, $S(k,0)$ [11]. The ratio $S(k,\tau)/S(k,0)$ and its decay time will be compared between theory and experiment below. A feature of $S(k,\tau)/S(k,0)$ is that it needs no correction due to the microscope's point spread function. Ratios of $S(k,\tau)/S(k,0)$ in the critical Ising model and in the mean-field approximation are similar, and do not depend strongly on correlation length, as will be shown in a future manuscript.

The HC model with $L_h = 6$ μm fits the data over all experimentally accessible wavenumbers. Fig. 3C shows the ratio $S(k,\tau)/S(k,0)$ at wavenumbers 1.1 μm^{-1} and 3.8 μm^{-1}. Fig. 3B shows decay times, defined as when $S(k,\tau)/S(k,0) = e^{-1}$. All other models are excluded. Fig. 3A rules out 2D Model H because the measured $z_{\rm eff}$ rises close to 3, well above the predicted value of 2 for 2D model H. Fig. 3B-C rules out 2D Model B because measured decay times are orders of magnitude shorter than the model predicts.

Developing Model HC to completely describe membranes requires determining only membrane viscosity, η_{2D}, as an input since the viscosity of water, η_{3D}, is known. Fig. 3C indicates that η_{2D} must be nonzero. In the small k limit, Inaura and Fujitani [11] predict a structure factor that depends only on η_{3D}. This parameter-free prediction, equivalent to taking $\eta_{2D} = 0$, underestimates time decays by a factor of $5-10$ (dashed curve, Fig. 3C). Setting the unknown η_{2D} (or equivalently, $L_{\rm h} = \eta_{2D}/\eta_{3D}$) as a single fit parameter within Model HC over the entire measured range of k yields $L_{\rm h} = 6.0 \pm 1.5$ μm. This value is within the range found by tracking diffusion of liquid domains across vesicle surfaces [21, 22] and is similar to values (2-4 μm) found by other methods, albeit for different lipid mixtures [23, 24]. An essentially equivalent method of finding $L_{\rm h}$ is to calculate the Model HC structure factor using the formalism of Hohenberg and Halperin [9], and to thereby extend Model HC to incorporate Ising rather than mean field statics. Within experimental uncertainty, this modest change has no effect ($L_{\rm h} = 5.5 \pm 1.5$ μm). This and other extensions of Model HC, each leading to small corrections to the ratio $S(k,\tau)/S(k,0)$, will appear in a future manuscript.

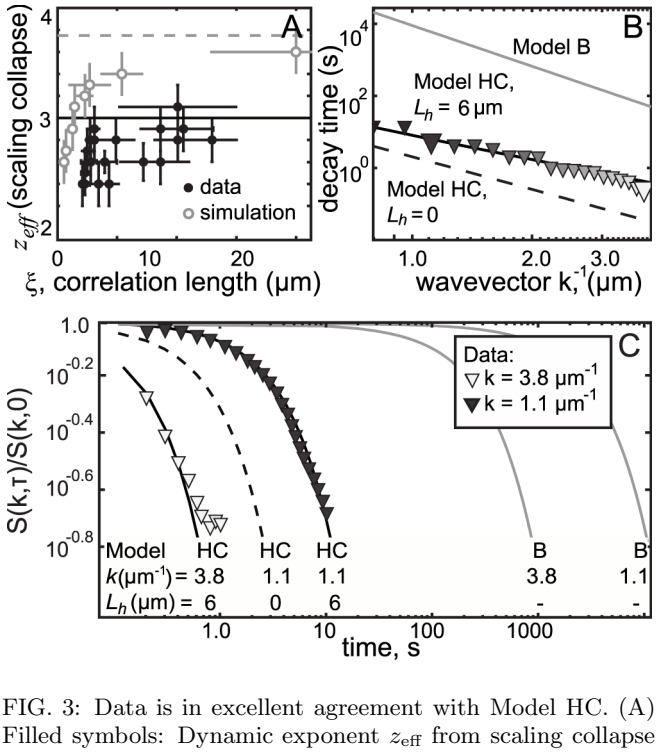

FIG. 3: Data is in excellent agreement with Model HC. (A) Filled symbols: Dynamic exponent $z_{\rm eff}$ from scaling collapse of experimental data as in Fig. 2A-B. Open symbols: Model B simulation in which $z_{\rm eff}$ approaches ~ 3.75. (B) Decay time, defined as when $S(k,\tau)/S(k,0) = e^{-1}$. Large symbols indicate wavenumbers 1.1 and 3.3 μm^{-1}. (C) Normalized structure factors $S(k,\tau)/S(k,0)$. In panels B and C, experimental data is denoted by symbols, 2D Model B by a grey line, Model HC (HC) with $L_{\rm h} = 6$ μm by a solid line and Model HC with $L_{\rm h} = 0$ by a dashed line.

Using lipid bilayers to measure critical exponents introduces both complexities and advantages, which are outlined further in [5]. The first complexity is that the simplest bilayers that exhibit critical phenomena contain ternary lipid compositions. Strictly speaking, the ternary mixtures used here pass through isothermal critical mixing (plait) points rather than critical (col) points. A feature of 2D systems is that, unlike in 3D systems, no measurable change in critical exponents arises from the presence of a third component. Briefly, a small correction to scaling arises in systems that contain a third component at fixed composition rather than fixed chemical potential. Hence, $T_{\rm c}$ changes, and many effective critical exponents are renormalized by a factor of $1/(1-\alpha)$, as discovered by Widom [25] and generalized by Fisher [26]. For the 2D Ising case here, where $\alpha = 0$, theory predicts only a logarithmic correction to singular behavior [25]. The second complexity is that when T is changed (as required in previous studies to find ν and β [3], but not required here), a bilayer with fixed composition does not necessarily follow a path with constant $\langle m(\vec{r})\rangle$ [27]. However, since membrane phase diagrams are relatively symmetric over the range of temperatures probed and since measured values of ν and β were consistent with the 2D Ising model [3], deviations from a path of constant $\langle m(\vec{r})\rangle$ are likely minor.

The first advantage of using lipid bilayers is that it avoids challenges of other systems. For example, lipid monolayers have confounding effects of dipole interactions, and the task of achieving simultaneous tunability and stability of surface pressure in a stationary monolayer is formidable. The second is that correlation lengths are large, partly because ξ_0 within the relation $\xi = \xi_0 \, |(T-T_c)/T_c|^{-\nu}$ is on the order of the length of a lipid molecule rather than of an atom. Separately, there

is an advantage in using 2D (or quasi-2D) experimental systems over 3D systems. The critical region is larger in 2D liquid-liquid critical systems than in analogous 3D ones, partially due to differences between critical exponents in 2D vs 3D Ising classes ($\nu = 1$ and $\beta = 1/8$ in 2D vs $\nu \approx 0.630$ and $\beta \approx 0.325$ in 3D [7]).

Methods used to produce the results in Fig. 3 follow. To optimize movie quality, vesicles were spherical, free-floating, unilamellar, of radius >100 μm, and electroformed by standard methods detailed in [3]. Vesicles were formed from mixtures along a line of plait points centered at 30% diphytanoylphosphatidylcholine (DiPhyPC), 20% dipalmitoylphosphatidylcholine (DPPC) and 50% cholesterol (chol), with 0.5% fluorescent dye Texas red dipalmitoylphosphatidylethanolamine (TR-DPPE). Only vesicles near a plait point were analyzed, identified by micron-scale composition fluctuations visible over the largest observed range of temperatures ($> 1°$C) and by equal areas of coexisting liquid phases below T_c. Each vesicle analyzed fell on a slightly different plait point, so each had a slightly different T_c [28].

Images of membranes were captured via an epifluorescence microscope with a temperature-controlled stage and a mercury lamp source. Light exposure was minimized by employing a SmartShutter (Sutter Instrument, Novato CA) controlled through NIS-Elements (Nikon, Melville NY) and by recording movies for at least two different frame rates at each temperature. Each frame was exposed 100-150 ms, with the shutter open 10 ms before and after exposures. Movies were collected from high to low temperature in steps of $\sim 0.2°$C, equilibrated for at least 2 min. No consistent trend in intensity was observed throughout each movie, implying that the low light procedures used here eliminated significant photobleaching. To correct for lamp flickering, mean brightness was subtracted from each frame. Spatial intensity gradients due to other vesicles outside the focal plane were removed by a long wavelength filter of 100 pixels.

Images were analyzed via custom MATLAB code (The Mathworks, Natick, MA). Vesicles were tracked and centered to remove drift (typically $< 25\mu m/$min). By eye, features exhibit no net translation, which implies no significant vesicle rolling. No difference in mean intensity or noise between pixels at edges vs. centers of cropped images was observed, implying that vesicles are so large that membrane curvature over images can be neglected [3]. Curvature corrections in smaller vesicles were minor [6].

The structure factor $S(k,\tau)$, the Fourier transform in space of the time-dependent correlation function, was found as previously described [3, 29]. Briefly, a discrete transform was performed for each movie image, with a buffer of zero values to correct for image non-periodicity. Transformed images were divided by the microscope's finite point spread function to yield $m(\vec{k},t)$. The dynamic structure factor was generated at each τ by $S(\vec{k},\tau) = 1/2\left\langle m(\vec{k},t)\overline{m(\vec{k},t\pm\tau)}\right\rangle$, where $\overline{m(\vec{k},t)}$ is the complex conjugate of $m(\vec{k},t)$ [30]. $S(\vec{k},\tau)$ was then radially averaged to yield $S(k,\tau)$.

Structure factors were employed in two ways. First, correlation lengths, ξ, were found by analyzing structure factors at $\tau = 0$. Specifically, a one-parameter fit for ξ was made until all data for $k^{(7/4)}S(k)$ vs. $k\xi$ collapsed onto the single curve for the exact numerical solution of the 2D Ising model [3, 31]. Second, effective dynamic scaling exponents, $z_{\rm eff}$, were found by collapsing curves of $S(k,\tau)$ (see results above and [5] for details). Collapse works because, according to the dynamic scaling hypothesis, structure factors within the scaling regime can be written in the form $S(k,\tau,\xi) = k^{-2+\eta}\Omega((k\xi)^{-1}, k^z\tau)$ where Ω is a universal function of $(k\xi)^{-1}$ and $k^z\tau$ [9]. Near T_c, where $(k\xi)^{-1}$ is near 0, curves of $S(k,\tau)/S(k,0)$ vs $k^z\tau$ collected over many wavenumbers k should collapse via a one-parameter fit to produce the correct value of z. Here, Ω can also depend on $kL_{\rm h}$, so that $S(k,\tau,\xi) = k^{-2+\eta}\Omega((k\xi)^{-1}, k^z\tau, kL_{\rm h})$. For collapses in Fig. 2A-B, $z_{\rm eff}$ refers to an effective z value which varies as $\xi/L_{\rm h}$ is changed. In Fig. 3B-C, comparing the entire form of the structure factor to theoretical predictions directly verifies the value of z as well as the dependence of the universal function on $kL_{\rm h}$ and $k^z\tau$.

Summary: Directly imaging composition fluctuations enables measurement of effective dynamic critical exponents of a lipid membrane embedded in bulk water. Experimental structure factors are in excellent agreement with an emerging theoretical prediction in which 3D hydrodynamics affects critical slowing down in a 2D membrane. The theory invokes hydrodynamic coupling between the membrane and bulk fluid such that Ising degrees of freedom are coupled to momentum modes [10, 11]. As predicted, a shift in $z_{\rm eff}$ from ~ 2 to ~ 3 as $T \to T_c$ and $\xi \to \infty$ is observed.

This work was supported by the NSF (MCB-0744852), a Molecular Biophysics Training Award (NIH 5 T32 GM08268-20), a UW Center for Nanotechno-logy IGERT (DGE-0504573), and NIH k99GM-087810. P. Cicuta kindly provided the domain-tracking Matlab routine [3] customized here. J.R. Ashcraft, M.E. Cates, R.E. Goldstein, M. Haataja, T. Lubensky, D.R. Nelson, M. den Nijs, P.D. Olmsted, G. Garbès Putzel, M. Schick, J.V. Sengers, J.P. Sethna, S.L. Veatch, B. Widom and A. Yethiraj are thanked for insightful conversations.

* Electronic address: slkeller@chem.washington.edu

[1] S. Veatch *et al.*, Proc. Natl. Acad. Sci. U.S.A. **104**, 17650 (2007).
[2] C. Esposito *et al.*, Biophys. J. **93**, 3169 (2007).
[3] A. Honerkamp-Smith *et al.*, Biophys. J. **95**, 236 (2008).
[4] A. Honerkamp-Smith, S. Veatch, and S. Keller, Biochim.

Biophys. Acta **1788**, 53 (2009).
[5] See EPAPS Document No. [number will be inserted by publisher] for movies and additional methods. For more information on EPAPS, see http://www.aip.org/pubservs/epaps.html .
[6] S. Veatch *et al.*, ACS Chem. Biol. **3**, 287 (2008).
[7] N. Goldenfeld, *Lectures on phase transitions and the renormalization group* (Addison-Wesley, NY, 1992).
[8] J. P. Sethna, *Statistical Mechanics: Entropy, Order Parameters, and Complexity* (Oxford Univ., Oxford, 2006).
[9] P. Hohenberg and B. Halperin, Rev. Mod. Phys. **49**, 435 (1977).
[10] M. Haataja, Phys. Rev. E **80**, 020902(R) (2009).
[11] K. Inaura and Y. Fujitani, J. Phys. Soc. Jpn. **77**, 114603 (2008).
[12] M. Dunlavy and D. Venus, Phys. Rev. B **71**, 144406 (2005).
[13] S. Casalnuovo, R. Mockler, and W. O'Sullivan, Phys. Rev. A **29**, 257 (1984).
[14] M. Yalabik and J. Gunton, Phys. Rev. B **25**, 534 (1982).
[15] B. Zheng, Phys. Rev. A **282**, 132 (2001).
[16] K. Kawasaki, Phys. Rev. Lett. **29**, 48 (1972).
[17] L. Kadanoff and J. Swift, Phys. Rev. **166**, 89 (1968).
[18] E. Siggia, B. Halperin, and P. Hohenberg, Phys. Rev. B **13**, 2110 (1976).
[19] P. Saffman and M. Delbruck, Proc. Natl. Acad. Sci. U.S.A. **72**, 3111 (1975).
[20] B. Hughes, B. Pailthorpe, and L. White, J. Fluid Mech. **110**, 349 (1981).
[21] P. Cicuta, S. Keller, and S. Veatch, J. Phys. Chem. B **111**, 3328 (2007).
[22] E. Petrov and P. Schwille, Biophys. J. **94**, L41 (2008).
[23] B. Camley *et al.*, Biophys. J. **99**, L44 (2010).
[24] R. Dimova *et al.*, Eur. Phys. J. B. **12**, 589 (1999).
[25] B. Widom, J. Chem. Phys. **46**, 3324 (1967).
[26] M. Fisher, Phys. Rev. **176**, 257 (1968).
[27] J.A. Zollweg and G.W. Mulholland, J. Chem. Phys.**57**, 1021 (1972).
[28] S. Veatch and S. Keller, Biochim. Biophys. Acta **1746**, 172 (2005).
[29] C. Takacs, G. Nikolaenko, and D. Cannell, Phys. Rev. Lett. **100**, 234502 (2008).
[30] D. Kolin, D. Ronis, and P. Wiseman, Biophys. J. **91**, 3061 (2006).
[31] T. Wu *et al.*, Phys. Rev. B. **13**, 316 (1976).